PERGAMON

Journal of Structural Geology 22 (2000) 1311–1324

JOURNAL OF STRUCTURAL GEOLOGY

www.elsevier.nl/locate/jstrugeo

Numerical simulation of fibre growth in antitaxial strain fringes ☆

Daniel Koehn[a,*], Chris Hilgers[b], Paul D. Bons[a], Cees W. Passchier[a]

[a]Institut für Geowissenschaften, Tectonophysics, Johannes Gutenberg Universität, Becherweg 21, 55099 Mainz, Germany
[b]Geologie-Endogene Dynamik, RWTH Aachen, Lochnerstrasse 4-20, 52056 Aachen, Germany

Received 28 June 1999; accepted 8 March 2000

Abstract

A two-dimensional computer model ('Fringe Growth') is used to simulate the incremental growth of crystal fibres in undeformed antitaxial strain fringes. The user can define the shape of a core-object (e.g. a pyrite crystal), the growth velocity and anisotropy of growing crystals, the rotation of fringes and core-object with respect to a horizontal datum and with respect to each other, and the opening velocity of fringes. Growth is simulated by movement of nodes connecting line segments that define the grain boundaries.

Modelling results predict that face-controlled strain fringes will grow around smooth core-objects and strain fringes with displacement-controlled and face-controlled fibres around core-objects with rough surfaces. The surface roughness of the core-object determines if fibres in the fringes track the opening trajectory, since fibres follow asperities on the surface of the core-object. Rotation of the core-object and the fringes with respect to an external reference frame and with respect to each other influences the geometry of the fibres. Our modelling results indicate that fibre growth direction is not directly dependent on the orientation of the extensional instantaneous stretching axes or the finite maximum strain axes. © 2000 Elsevier Science Ltd. All rights reserved.

1. Introduction

Rigid objects in a matrix deformed by non-coaxial or coaxial progressive deformation cause perturbations of the stress field and flow pattern. Increased pressure solution may occur adjacent to the rigid object on the side of the shortening instantaneous stretching axes (ISA), while new crystals may grow on the side of the extensional ISA and form strain fringes (Mügge, 1928; Pabst, 1931). For over 70 years, geologists have attempted to use crystal fibres in strain fringes that lie on both sides of a rigid core-object such as a pyrite crystal to evaluate the deformation history in the host-rock (Mügge, 1928; Pabst, 1931; Durney and Ramsay, 1973; Cox and Etheridge, 1983; Beutner and Diegel, 1985; Ellis, 1986; Etchecopar and Malavielle, 1987; Aerden, 1996; Kanagawa, 1996). Despite much progress in this field, the methods used are still based on assumptions which have not been tested experimentally. We developed a method to test assumptions of fringe growth in numerical experiments in order to improve the reliability of these structures as providers of kinematic data. The basic assumptions and problems of existing models are outlined below.

Fibre growth in fringes takes place either syntaxially at the matrix–fringe interface or antitaxially at the interface of the core-object and the fringe, and fibres may or may not deform during ongoing deformation (reviews in Ramsay and Huber, 1983; Passchier and Trouw, 1996). This study deals with undeformed antitaxial strain fringes that are most common in nature. Fig. 1 shows examples of such antitaxial non-deforming strain fringes. The core-object can be a spherical framboidal pyrite (Fig. 1a) or an angular iron-oxide object (Fig. 1b). Both examples are inferred to have developed during progressive non-coaxial deformation with a dextral shear sense (Passchier and Trouw,

☆ Figs. 6–8 visible as Quick Time movies on http://veo.elsevier.nl/sg/Publish/925.

* Corresponding author.
E-mail address: koehn@mail.uni-mainz.de (D. Koehn).

0191-8141/00/$ - see front matter © 2000 Elsevier Science Ltd. All rights reserved.
PII: S0191-8141(00)00039-0

1996). Two models have been proposed in the literature for the development of antitaxial strain fringes, and according to these models the fibres in the fringes may grow in a direction controlled by the orientation of the surface of the core-object (face-controlled growth) or they may grow parallel to the opening trajectory of the fringe irrespective of core-object orientation (displacement-controlled growth) (reviews in Ramsay and Huber, 1983; Passchier and Trouw, 1996).

Strain fringes that are inferred to be displacement-controlled have been used to evaluate incremental and finite strain histories (Durney and Ramsay, 1973; Beutner and Diegel, 1985; Ellis, 1986; Etchecopar and Malavielle, 1987; Aerden, 1996; Kanagawa, 1996). Several authors have stated that single displacement-controlled fibres can be used to evaluate the incremental orientation of the extensional ISA with respect to an external reference frame (e.g. the Earth's surface) (Durney and Ramsay, 1973; Ramsay and Huber, 1983;

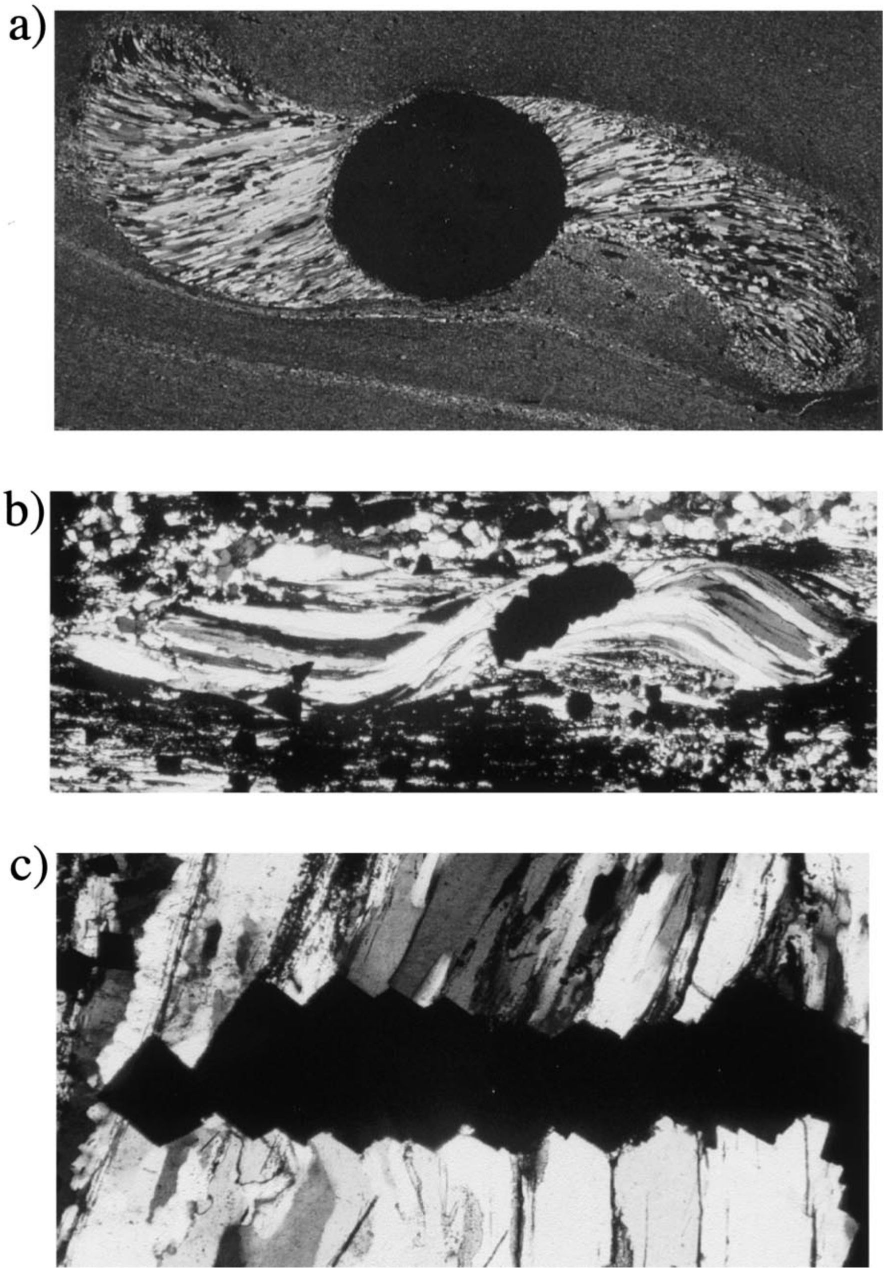

Fig. 1. (a) Micrograph of quartz fringes adjacent to a framboidal pyrite that developed during progressive non-coaxial deformation with a dextral shear sense, Leonora, Yilgarn Craton, Australia. Width of view is 20 mm. (b) Micrograph of quartz strain fringes adjacent to an elongate iron oxide core-object from the Hamersley Ranges, Australia that developed during progressive non-coaxial deformation with a dextral shear sense. Width of view is 8 mm. (c) Micrograph of quartz fibres adjacent to a rough iron oxide core-object from the Hamersley Ranges, Australia. Fibre boundaries are locked to outward-pointing asperities on the core-object surface. Width of view is 3 mm.

Beutner and Diegel, 1985; Ellis, 1986; Etchecopar and Malavielle, 1987; Aerden, 1996). Aerden (1996) has shown that this assumption is only valid for fibres in a plane cut parallel to the extensional ISA for coaxial progressive deformation if the core-object is not rotating with respect to its fringes. Rotation of the core-object with respect to its fringes will influence the geometry of fibres so that their long axis is no longer parallel to the extensional ISA (Aerden, 1996). The core-object in strain fringes will rotate with respect to ISA during (1) coaxial progressive deformation if it is elongate and not aligned with its long axis parallel to the extensional ISA or (2) non-coaxial progressive deformation (Ghosh and Ramberg, 1976; Aerden, 1996).

Non-coaxial progressive deformation produces complex fibre and fringe geometries which are difficult to interpret (Etchecopar and Malavielle, 1987; Aerden, 1996; Kanagawa, 1996; reviews in Passchier and Trouw, 1996). If the Earth's surface is used as an external reference frame during non-coaxial progressive deformation, the finite strain axes, fringes and core-object may all rotate with respect to this reference frame (Aerden, 1996; Passchier and Trouw, 1996; Fig. 2). The orientation of the extensional ISA cannot be determined easily from strain fringes in this case, since the influence of the fringe- or object-rotation on fibre geometry is not clear. Nevertheless, several authors use specific assumptions to interpret matrix deformation from strain fringes (Beutner and Diegel, 1985; Ellis, 1986; Etchecopar and Malavielle, 1987; Aerden, 1996; Kanagawa, 1996). Beutner and Diegel (1985) do not consider fringe and core-object rotation with respect to an external reference frame; Ellis (1986) treats fringes and core-object as one rotating complex with respect to an external reference frame. Etchecopar and Malavielle (1987) and Kanagawa (1996) include different rotational behaviour of fringes and core-object in their methods. Aerden (1996) developed a method that can determine the rotation of fringes and core-object. He tried to trace sudden changes in the orientation of the extensional ISA with respect to an external reference frame, which he interprets in terms of polyphase deformation.

The methods described above are based on different assumptions regarding the mechanism of fibre growth. In order to interpret strain fringes in a reliable way it is necessary to test these assumptions and to explain why fibres grow face- or displacement-controlled. Urai et al. (1991) developed a model that links growth of fibres to the presence of asperities on the surface of a core-object. They pointed out that when a polycrystalline fringe is pulled away from a core-object with asperities, the growth surface will be an irregularly shaped cast of the core-object. A simple geometrical consideration shows what happens if fibres grow equally fast and fill small 'cracks' formed when fringe and core-objects are pulled apart by several small steps: fibre boundaries will end up 'fixed' to the tips of embayments in the irregular growth surface that point in the direction of the fringe. Therefore, the fibres are effectively 'fixed' to the tips of asperities that fit in the embayments (Fig. 3). We developed a computer program 'Fringe Growth' based on the theory of Urai et al. (1991) to model the growth of fibrous crystals in antitaxial strain fringes. The program can model differently shaped core-objects with different surface roughness to investigate the growth of face-controlled and displacement-controlled fibres during progressive coaxial deformation with straight fringe opening paths. We also tried to mimic progressive non-coaxial deformation using curved fringe opening paths and rotation of the core-object with respect to the fringes. We investigated the progressive fibre growth patterns during these experiments to test if the growth hypothesis of Urai et al. (1991) can explain fibre patterns examined in natural non-deforming antitaxial strain fringes. We

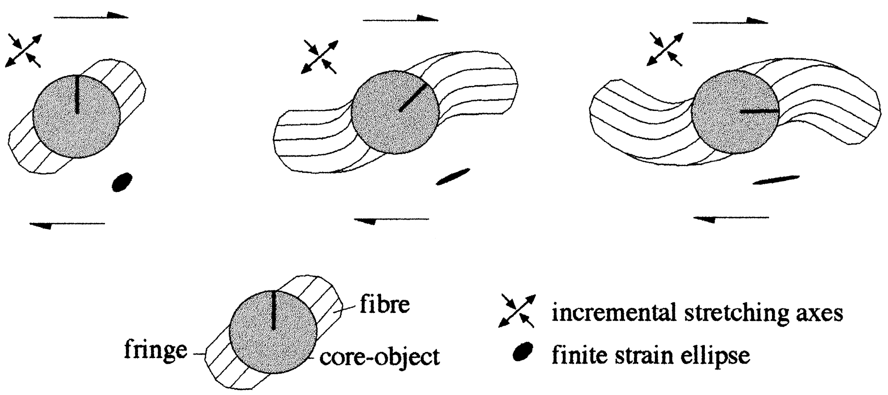

Fig. 2. Schematic illustration of the development of a fibrous strain fringe in simple shear, after Aerden (1996) and Passchier and Trouw (1996). Both the fringes and the core-object rotate with respect to ISA and the flow plane.

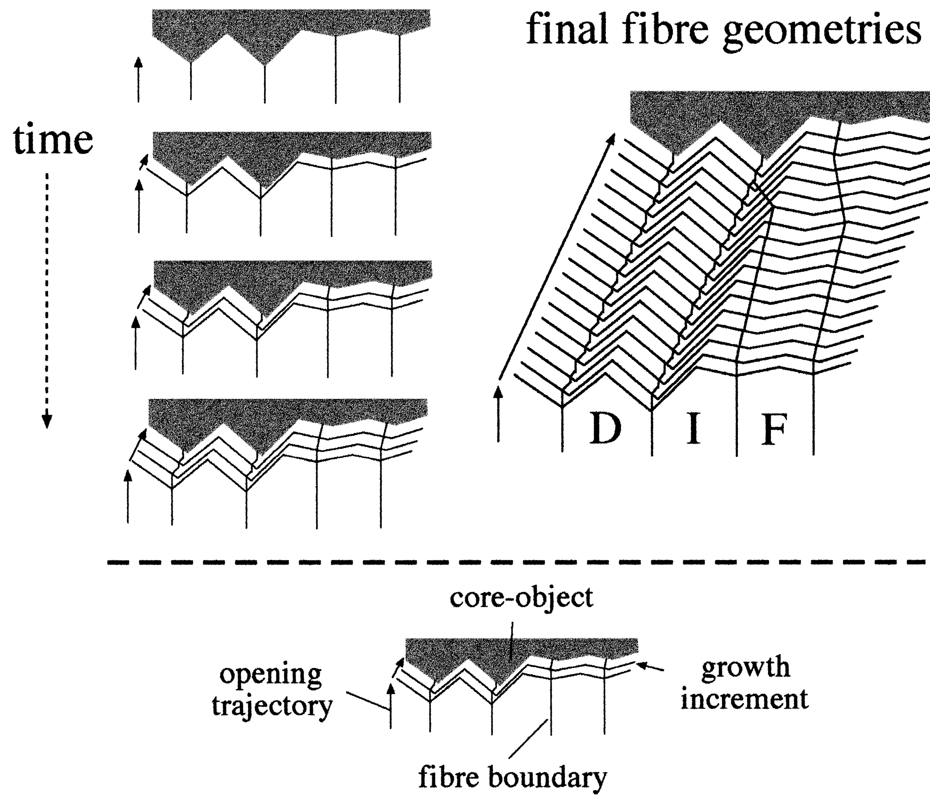

Fig. 3. Figure showing the tracking capability of outward-pointing asperities after Urai et al. (1991). D = displacement-controlled fibre, I = intermediate fibre, F = face-controlled fibre. Fibres grow isotropically so that fibre boundaries are oriented perpendicular to the growth surfaces. If the opening path of the core-object is not perpendicular to the enveloping surface of the core-object, fibre boundaries will first grow straight. They are now oriented at one side of the asperity and will grow back towards its tip if the asperity is pronounced enough. This process will produce tracking fibre boundaries.

discuss the implications of this growth hypothesis on commonly used kinematic analysis of antitaxial strain fringes.

2. The computer model

The computer model 'Fringe Growth' is based on the algorithm of the model 'Vein Growth' by Paul Bons (Bons, in press) and is written in 'C' for Macintosh. 'Fringe Growth' simulates two-dimensional growth of fibrous grains in one of the two fringes adjacent to a rigid core-object. The horizontal and vertical axes of the computer screen are used as an internal reference frame (Fig. 4). The fringe is fixed in this reference frame and only the core-object can move and rotate with respect to the fringe. Fibrous grains that build the fringe grow towards the core-object at the object–fringe interface so that the fringes are of the antitaxial type (Fig. 5). The growth rate of the crystals, the opening rate and opening direction of the fringe and the rotation of the core-object around its centre are independent of each other and can be defined by the user. The model is only simulating the fibre growth process; the matrix around the strain fringe is not

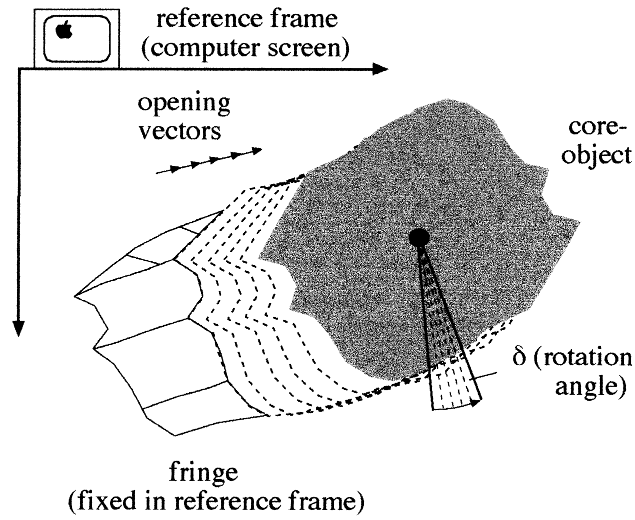

Fig. 4. Diagram showing how the core-object is moved in the 'Fringe Growth' program. The fringe is fixed in an internal reference frame (the computer screen). The opening vector defines the magnitude and direction of the core-object movement. The rotation angle δ describes rotation of core-object around its centre relative to the computer's reference frame and to the fringe.

included in the simulations. The contact of the fringe to the matrix is the boundary of the model. Once grains have nucleated on this boundary, the boundary remains stable since the fringes are not deforming. Any core-object shape can be created by the user from digitised drawings. Four pre-defined shapes are available: smooth square, rough square, smooth round and rough round core-objects. The program inserts the first grains with a user-defined width at the rim of the core-object where the fringe opens. A growth-anisotropy of the crystals in the fringe can be defined by a two-dimensional crystal growth file (Bons, in press). The growth anisotropy defines the crystal growth habit or euhedral shape. For our simulations we use a prismatic mineral growth file (Bons, in press).

2.1. Growth of fibrous grains

The grains in the fringe, the fringe itself and the core-object are polygons defined by a number of nodes (Fig. 5). These polygons are all connected with each other. Triple junction nodes connect three neighbouring nodes and are on the vertices of three polygons; double junction nodes connect two neighbouring nodes and lie between two neighbouring polygons. During runtime, nodes are moved by small increments that are calculated from the maximum growth velocity defined by the user and from the orientation of the growth surface with respect to the crystallographic orientation of the grain (Fig. 5). A detailed description of the growth algorithm is given in Bons (in press). If the distance between two nodes is below a user-defined critical value, one node is removed; if the distance is above this critical value an extra node is added. This keeps the user-defined distance between nodes roughly constant. Following an opening step of the fringe, nodes of growing grains are unlocked and grow until they reach the core-object (Fig. 5). Then they are locked until the fringe opens again. Nucleation of new grains takes place at the contact of the fringe with the matrix (the boundary of the model) (Fig. 5). The program will insert a new nucleus if the grain next to the fringe has reached a user-defined width. Sometimes large new sections of a fringe can open at once, especially if the core-object has pronounced corners. If there is enough space for more than one nucleus, the program will keep on nucleating crystals until the free space is filled.

2.2. Movement of the core-object

In our model, fringes are fixed in the internal reference frame and fibre-geometry in a developing fringe is completely defined by movement of the core-object. This movement has two components: (1) displacement of its centre away from the fringe and (2) rotation around the object centre. Both are varied in our experiments. The movement of the centre of the core-object away from the fixed fringe is described by the magnitude and direction of the opening vector per time increment (Fig. 4) as defined by the user and is termed the object-centre path. The computer screen is used as a reference frame for the direction of the opening vector. The user can change the magnitude and direction of the opening vector and can also define a permutation angle by which the direction of the opening vec-

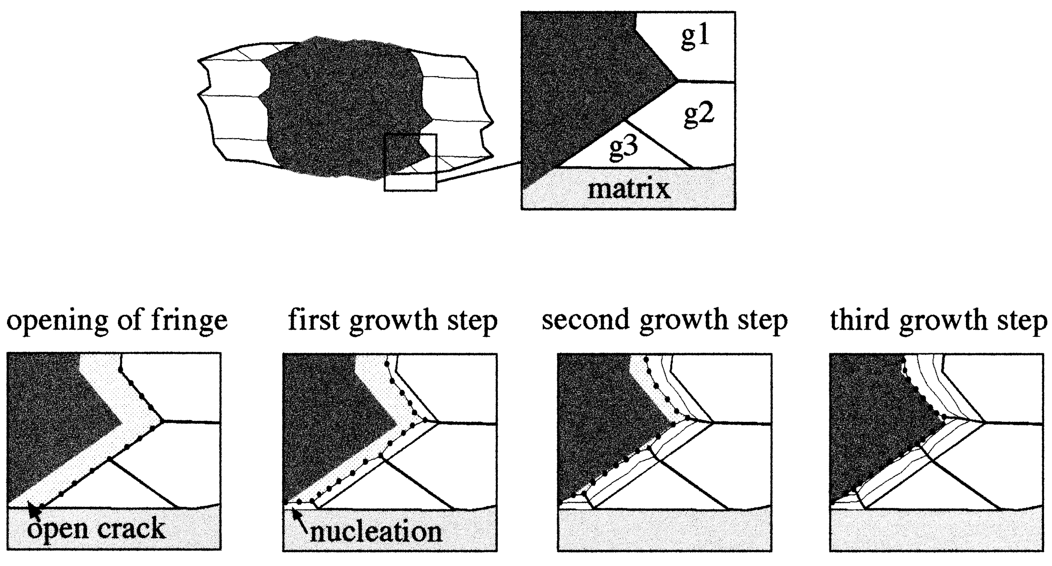

Fig. 5. Schematic illustration of the way in which fibres grow in the computer program. g1, g2 and g3 are fibres in the fringe. Once the fringe opens (movement of the core-object) nodes on the grain boundaries will move resulting in fibre growth towards the core-object until the free space is filled. A new nucleus is inserted next to the rim of the fringe after the fringe has opened.

tor will change at each opening increment. This produces curved object-centre paths. The core-object can rotate by user-defined amounts around its centre with respect to the computer's reference frame. Anticlockwise core-object rotation is positive and clockwise rotation negative. The program saves a picture of the growing fringe for every user-defined number of growth steps, so that movies of incremental fibre growth can be created.

3. Modelling results

Systematic runs of the program have been carried out with different core-object shape, core-object surface morphology, opening direction (object-centre paths) and relative core-object fringe rotation. The results show that face-controlled and displacement-controlled fringes are end-member cases as predicted by Urai et al. (1991). Face-controlled fringes develop around smooth core-objects, but around rough core-objects fringes are not always displacement-controlled since they contain both face- and displacement-controlled fibres (Fig. 6). Even single fibres switch from face- to displacement-controlled growth and vice versa, which is often observed close to changes of the object-centre path (Figs. 7 and 8). The results of the numerical modelling are discussed in the following sections.

3.1. Straight object-centre paths

We use straight object-centre paths to mimic coaxial

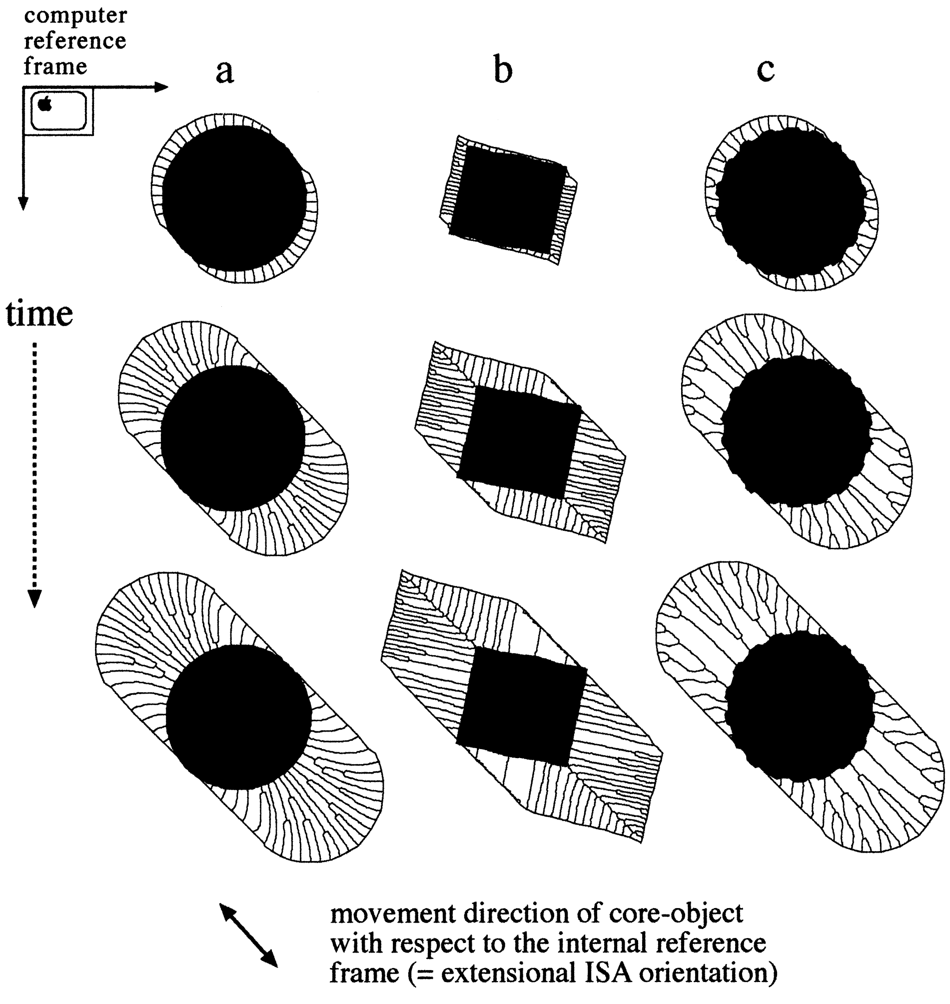

Fig. 6. Simulations of 'Fringe Growth' mimicking coaxial progressive deformation (straight object-centre paths) with ISA fixed in the internal reference frame and using different core-object shapes. Double fringes are shown to allow comparison with natural objects, although only one is modelled in the computer program. ISA orientation is parallel to movement direction of the core-object. (a) Simulation using a smooth round core-object. All the fibres grow face-controlled. The fibres show a curvature towards the centre of the core-object. (b) Simulation using a smooth square core-object. The fibres grow face-controlled towards the flat faces of the core-object. Displacement-controlled suture lines separate face-controlled fibres that grow in different directions. (c) Simulation with a rough round core-object. Most fibres grow displacement-controlled. Only fibres on the rims of the core-object grow face-controlled. The fibre width is dependent on the distance between the asperities on the core-object surface. (Figure visible as QuickTime movie on http://veo.elsevier.nl/sg/publish/925.)

progressive deformation without fringe rotation with respect to an external reference frame. In this case ISA are fixed in the external reference frame and in the computer reference frame (Fig. 6).

Face-controlled fibres around round core-objects with a smooth surface were found to develop in a geometry predicted by Passchier and Trouw (1996). All the fibres grow permanently towards the centre of the core-object (Fig. 6a). The fibres tend to get thinner and disappear after they have reached a certain length because fibres grow radially inwards towards the core-object. The fringes are symmetric with respect to a plane through the middle of the fringe and through the centre of the core-object (Fig. 6a). The fibres in the fringe develop a curved shape because the orientation of their growth surface changes as they grow from the rim of the fringe towards its centre (Fig. 6a).

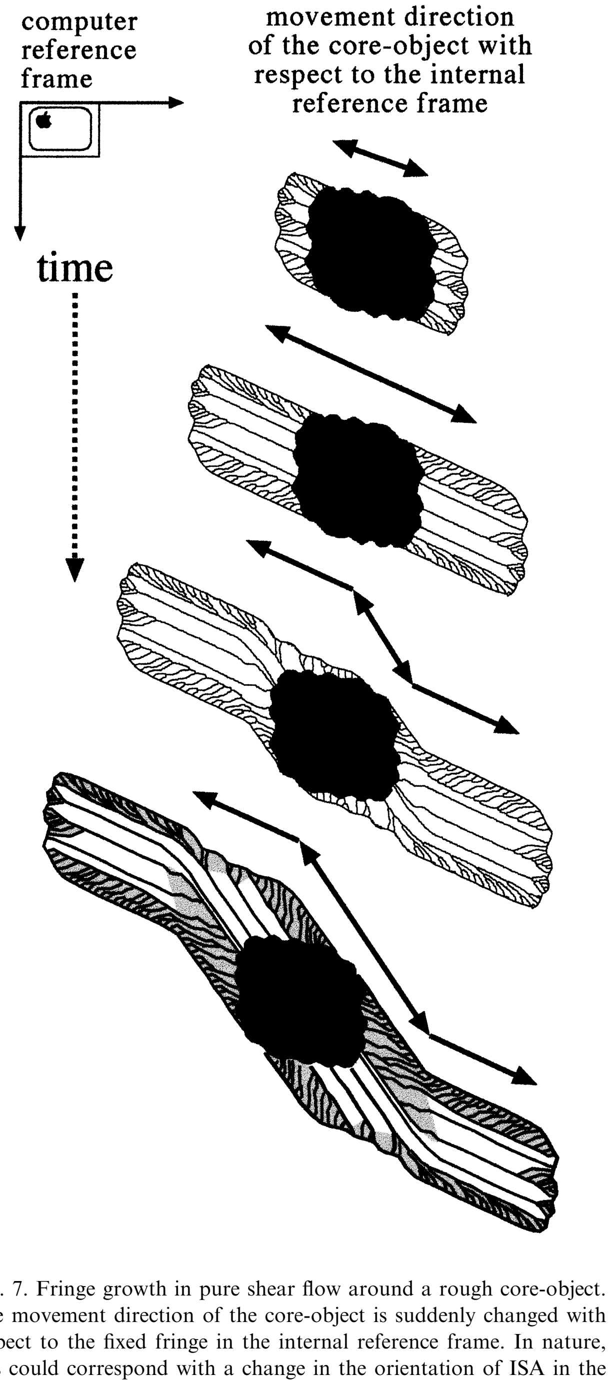

Fig. 7. Fringe growth in pure shear flow around a rough core-object. The movement direction of the core-object is suddenly changed with respect to the fixed fringe in the internal reference frame. In nature, this could correspond with a change in the orientation of ISA in the external reference frame. During a change of the opening trajectory some displacement-controlled fibres start to grow face-controlled and vice versa. In the final fringes, face-controlled fibre parts are marked grey and displacement-controlled fibre parts are white. Double fringes are shown to allow comparison with natural objects, although only one is modelled in the computer program. (Figure visible as QuickTime movie on http://veo.elsevier.nl/sg/publish/925.)

If the core-objects are square and have a smooth morphology, the fibres grow face-controlled perpendicular to the sides of the square (Fig. 6b). A suture line (Ramsay and Huber, 1983), which separates differently oriented face-controlled fibres, develops from the corners of the square core-object. The corners have the same effect on suture lines as small asperities on the surface of a rough core-object have on individual displacement-controlled fibre boundaries (Fig. 6c). This is valid for all core-objects: as soon as the core-object has corners, suture lines get trapped on these corners and become displacement-controlled.

If the core-object has a rough surface, outward-pointing asperities on the core-object tend to capture grain boundaries and create displacement-controlled fibres as predicted by Urai et al. (1991) (Figs. 1c and 6c). Whether or not fibre boundaries get locked on these asperities depends on the form of the asperities (amplitude and wavelength/amplitude ratio), on the orientation of the enveloping surface on which the asperities are located with respect to the opening vector, and also on the opening velocity of the fringe with respect to the growth velocity of the crystals (Urai et al., 1991). The tracking capability of asperities is described in detail in Section 3.3. Not all fibres in the fringes grow displacement-controlled since face-controlled fibres develop at the rims of the fringes where asperities are unable to lock fibre boundaries (Fig. 6c).

The width of the growing fibres is directly influenced by the distance between outward-pointing asperities on the core-object surface (Figs. 1c and 6c). If the asperities are close together, the fibres are thin. If they are further apart, fibres are thicker and fewer fibres develop. The size of the original nuclei only influences the width and number of the fibres if the nuclei are larger than the distance between the asperities (Hilgers et al., in press).

3.2. Object-centre paths with changing directions

Fibre patterns in strain fringes are most complex if the object-centre path is not straight and progressive deformation is non-coaxial. We tried to investigate two different scenarios. (1) The object-centre path is straight but changes suddenly during deformation by about 30° (Fig. 7). This either mimics a rigid body rotation where the strain fringes rotate suddenly with respect to ISA or a sudden rotation of ISA with respect to the strain fringes fixed in the external reference frame (e.g. polyphase deformation). (2) The object-centre path is curved. This mimics a progressive non-coaxial deformation, for example simple shear, where strain fringes are progressively rotating with respect to ISA fixed in the external reference frame (Figs. 8 and 9). In nature, this rotation of the fringes is due to the fact that they are rigid objects, and therefore subject to a torque associated with the vortical flow in the matrix. We also try to investigate displacement-controlled fibre patterns that are produced by relative core-object fringe rotation (Fig. 9).

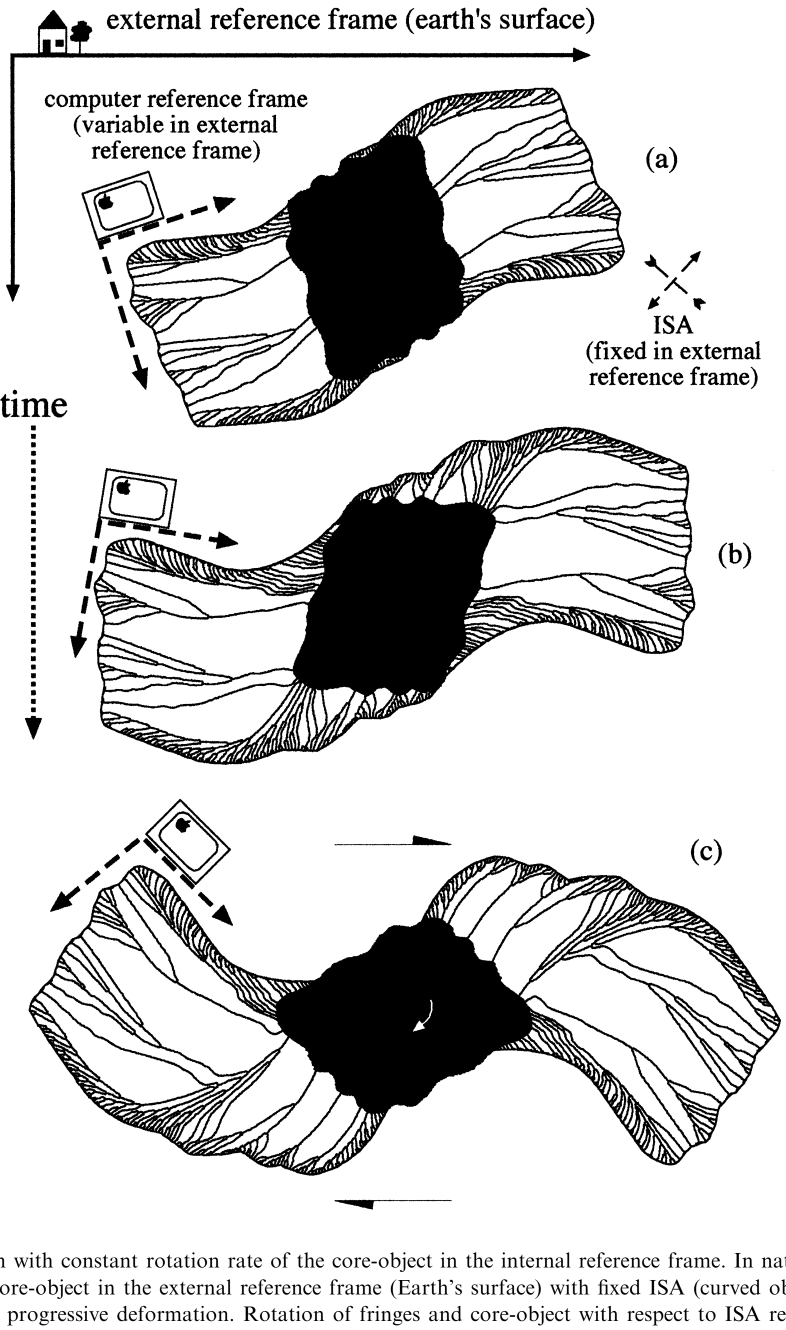

Fig. 8. Model of fringe growth with constant rotation rate of the core-object in the internal reference frame. In nature, this could correspond to rotation of both fringes and core-object in the external reference frame (Earth's surface) with fixed ISA (curved object-centre path). This model serves to simulate non-coaxial progressive deformation. Rotation of fringes and core-object with respect to ISA result in complex fibre patterns and fringe forms. None of the fibres grow parallel to the opening trajectory of the fringe. If a pronounced corner of the core-object rotates into the fringe the fibre patterns change completely and a suture develops. The fringe looks as if it experienced two different opening events. Note that the reference frame of the computer is rotating with respect to the external reference frame (Earth's surface) because the fringes are fixed in the computer reference frame. Double fringes are shown to allow comparison with natural objects, although only one is modelled in the computer program. (Figure visible as QuickTime movie on http://veo.elsevier.nl/sg/publish/925.)

Complex fibre geometries develop where we mimic changes in orientation of ISA with respect to the computer screen (internal reference frame) during a simulation. Displacement-controlled fibres may change to grow face-controlled and vice versa (ornamentation in Fig. 7). Such fibres containing face- and displacement-controlled parts are named '*intermediate fibres*'. It is therefore dangerous to use single fibres for a kinematic analysis, since fibres are not necessarily displacement-controlled along their whole length. The two different fibre types can be distinguished in Fig. 7 because the change in the direction of the object-centre path is sudden and pronounced (30°) and the core-object is not rotating with respect to the fringe. If the change in the direction of the object-centre path is more gradual and the core-object is rotating with respect to the fringe it can be very difficult to distinguish between displacement- and face-controlled fibres (Fig. 8).

If object-centre paths are curved, complex face- and displacement-controlled fibre-patterns develop. This is shown in Fig. 8 in three steps. Face-controlled fibres are common on the rims of the fringes. Displacement-controlled fibres develop from face-controlled fibres and are locked to outward-pointing asperities on the core-object surface (Fig. 8a). These displacement-controlled fibres change to grow face-controlled again during Fig. 8(b). New displacement-controlled fibres develop towards asperities on another face of the core-object during Fig. 8(c). It is difficult to distinguish face-controlled parts of fibres from displacement-controlled parts even in the experiments. In nature, where

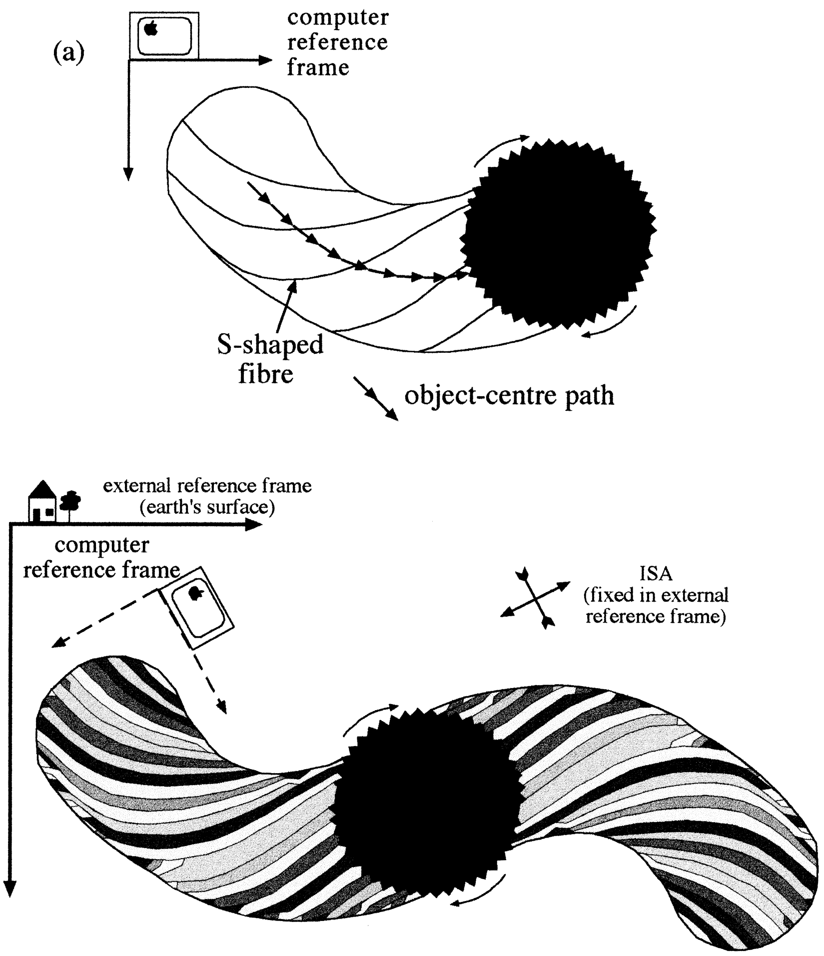

Fig. 9. Simulation of a fringe around a rough round core-object during non-coaxial progressive deformation. (a) In the computer model, the core-object rotates 90° with respect to the fixed fringe and the opening path is curved. Relative core-object fringe rotation produces a changing fibre curvature so that the fibres develop an S-form. Displacement controlled fibres are truncated by the rim of the fringe. (b) Double fringes are shown to allow comparison with natural objects, although only one is modelled in the computer program. In nature, the fringes and the core-object are inferred to rotate at different velocities with respect to the external reference frame (Earth's surface), so that core-object and fringes rotate relative to each other. The simulated fibre patterns are similar to the fibre patterns in Fig. 1(a). This suggests that in nature round core-objects do rotate with respect to their fringes.

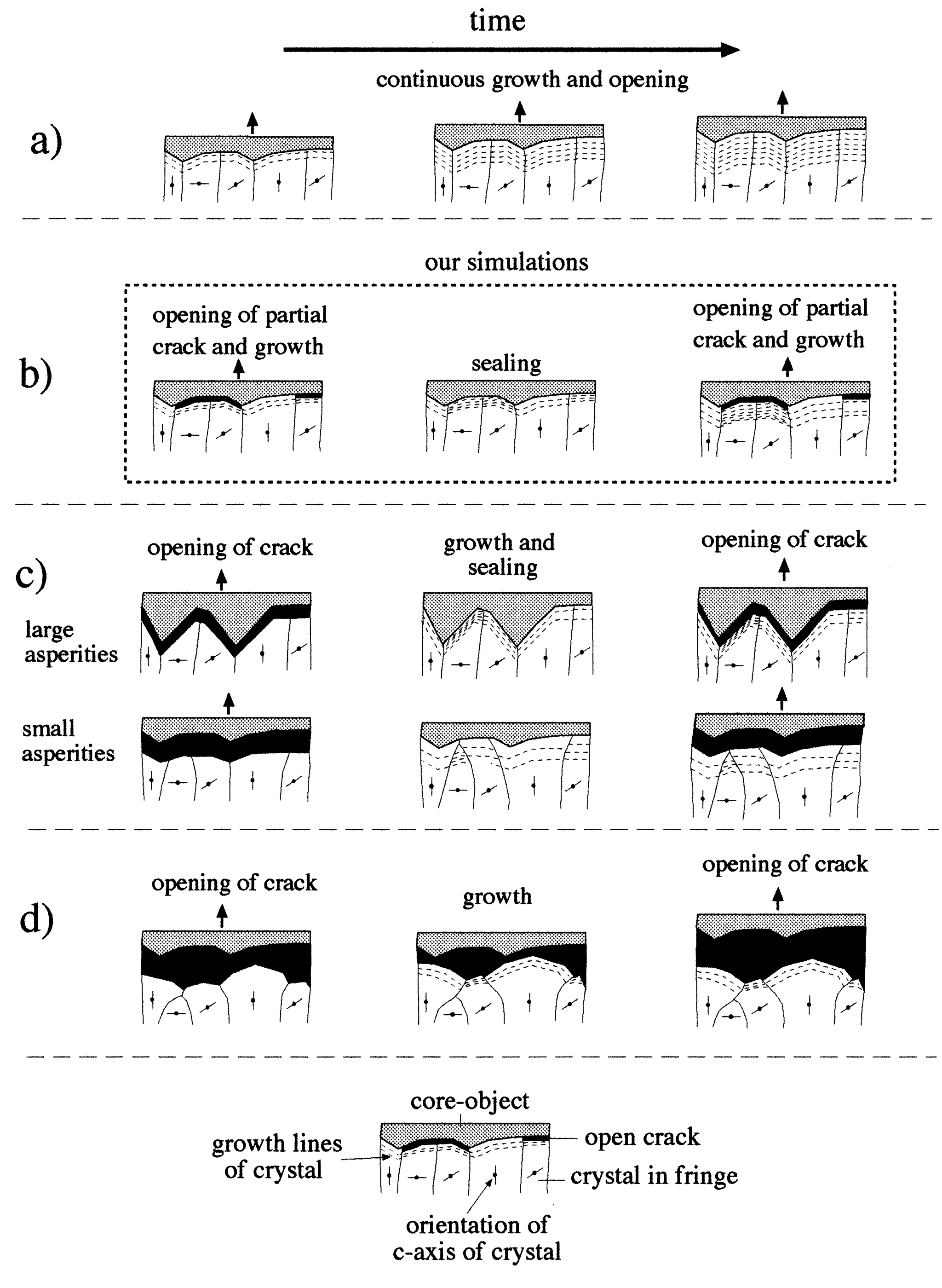

Fig. 10. Diagram showing the effect of four different opening rates of the fringe with respect to the growth rate of the growing crystals. (a) A single opening step of the fringe is smaller than the growth step of the slowest growing crystals. Growth and opening process is continuous. (b) A single opening step of the fringe is between the growth step of the slowest- and fastest-growing crystal. Crystals that are oriented with their slowest growth direction perpendicular to the growth surface are detached from the core-object and grow into small cracks. (c) A single opening step of the fringe is larger than the growth step of the fastest-growing crystal, but the crystals seal the open space before the next opening event. The crystals grow in a crack–seal manner and start to form crystal facets as they grow into open space (fluid-filled crack). A crack develops between the fringe and the core-object. Crystals may lose their tracking capability depending on the width of the crack compared to the size of the asperities on the surface of the core-object. The crystals will lose their fibrous habit and grow elongate or blocky if the crack width is too large. (d) The core-object is permanently completely detached from the fringe as the crystals do not grow fast enough to seal the open space. The crystals develop facets and have an elongated or blocky form.

progressive fringe development is not known but only the final geometry of the fibres can be studied, it is in many cases impossible.

Another variable which may be important in fringe development is rotation of the core-object with respect to the internal reference frame, i.e. the fringe. Fig. 9 shows simulation of a strain fringe around a rough round core-object. The object-centre path is curved and the core-object is rotated clockwise with respect to the growing fringe. In this experiment, we tried to reproduce the fibre patterns of Fig. 1(a). If the core-object is rotating with respect to the fringes, the curvature of displacement-controlled fibres will change progressively from one side of the fringe to the other and will have a geometry showing an S-shape during dextral progressive simple shear deformation (Fig. 9). This geometry cannot be generated using curved object-centre paths without core-object rotation: it only forms if the core-object has rotated with respect to the fringe, in the case of Fig. 9 by about 90°. The fibres are truncated by the rim of the fringe because of the curved object-centre path and the relative rotation of core-object and fringe. Displacement-controlled fibres in the fringe do not grow parallel to the extensional ISA (Fig. 9). As can be seen from comparison of Figs. 1(a) and 9(a), the geometry of the natural object closely resembles the modelled one, which suggests that the fringe in Fig. 1(a) formed during progressive non-coaxial deformation.

3.3. Tracking capability of outward-pointing asperities

The tracking capability of outward-pointing asperities as postulated by Urai et al. (1991) has been defined for isotropically growing crystals. During isotropic growth all the fibres in a fringe will grow with the same growth speed so that grain boundaries will always be perpendicular to the growth surface of the fibres. Fig. 3 illustrates how fibre boundaries of isotropically growing fibres can get captured by outward-pointing asperities according to Urai et al. (1991). In our simulations we use anisotropic growth kinetics, which are more realistic to model natural crystal growth. The opening velocity of the fringe with respect to the growth velocity of the crystals influences the shape of the crystals and their ability to track displacement. If we consider opening to occur by periodic steps, four different cases can be distinguished (Fig. 10) (Mügge, 1928); (a) a single opening step of the fringe is smaller than the incremental growth step of the slowest growing crystal; (b) a single opening step of the fringe lies between the incremental growth step of the slowest- and fastest-growing crystal; (c) a single opening step of the fringe is larger than the incremental growth step of the fastest-growing crystal, but the crystals are growing faster than the average opening velocity; (d) a single opening step of the fringe is larger than the incremental growth step of the fastest-growing crystal, and the crystals are growing slower than the average opening velocity of the fringe. In case (a) the crystals have no space to develop crystal facets: they will grow mostly isotropically so that their growth velocity is the same in every direction and will have excellent tracking capabilities as grain boundaries are mostly oriented perpendicular to the growth surface (Figs. 3 and 10a). In this way, the fringe develops continuously in a thin gap along the core-object if we consider that periodic opening steps are infinitesimally small. In case (b) the crystals tend to grow anisotropically because they grow partly into larger open cracks, and start to develop crystal facets because their growth velocity depends on the orientation of the growth surface with respect to the crystallographic orientation of the crystal (Fig. 10b). This reduces

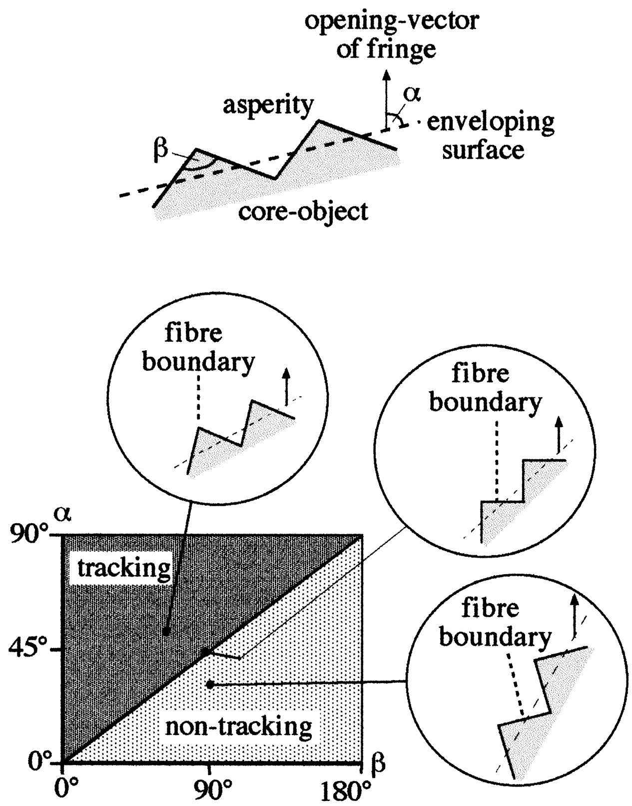

Fig. 11. Asperities can lock fibre boundaries depending on the shape (pointedness) of the asperities and the orientation of the enveloping core-object surface with respect to the opening direction. The pointedness of the asperities is described by the angle β of the asperity. The angle α describes the orientation of the core-object surface with respect to the opening-vector of the fringe. Asperities are able to lock fibre boundaries if $\alpha > \beta/2$. Asperities with an angle β of 180° are flat surfaces so that fibre boundaries cannot be locked. Very pointed asperities with an angle β approaching 0° will be able to lock fibres irrespective of α.

their tracking capability as the growth of grain boundaries is not necessarily perpendicular to the growth surface and the fibres may not be locked on the asperities anymore if these are small with respect to the growth steps of the crystals (Fig. 10b). We have tried to simulate case (b) by using an opening vector for incremental fringe opening that is smaller than an incremental growth step of the fastest-growing crystal. In case (c) a crack develops between the core-object and the fringe (Fig. 10c, d). If the crystals grow fast enough, they seal this crack before the next opening event. This 'crack–seal' process (Ramsay, 1980) reduces the tracking capability of crystals since they grow anisotropically. Fibres in the fringe will only follow asperities on the core-object if the crystals do not outgrow each other too quickly (Fig. 10c) and then lose their fibrous habit to grow elongate or blocky (Fisher and Brantley, 1992; Bons and Jessell, 1997). Once the crystals are not growing fast enough to seal the crack (case d) they grow anisotropically, lose all abilities to track displacement and develop elongate or blocky crystals instead of fibres (Fig. 10d). From case (a) to (d) crystals in fringes show a decreasing ability to track displacement, even if the core-object is rough. Cases (a), (b) and partly (c) may produce very similar structures depending on the anisotropy of the crystals and the roughness of the crack/growth surface.

If the opening of the fringe is a continuous process (case a) a simple diagram illustrates which asperities will lock fibre boundaries (Fig. 11) (Urai et al., 1991). The two important parameters are the angle β of the asperity (pointedness) and the angle α of the enveloping core-object surface on which the asperity is located with respect to the opening direction of the fringe (Fig. 11). The angle β is defined in Urai et al. (1991) as $2\arctan(\lambda/2y)$, where λ is the wavelength of the asperities on the core-object surface and y is the amplitude. The angle α is defined in this paper in a different way from Urai et al. (1991) who define α for veins as the angle between the local orientation of the crack surface and the opening vector so that α is dependent on β. In our case the two angles are independent, which simplifies an α–β diagram showing the tracking capability for fibres in strain fringes around core-objects. Using our definition, the asperities will be able to lock the fibre boundaries as long as $\alpha > \beta/2$. If $\alpha = \beta/2$, one side of the asperity will be at 90° to the growing fibre boundary (Fig. 11). If $\alpha > \beta/2$, the fibre boundary is locked to the asperity and if $\alpha < \beta/2$ the fibre boundary will grow away from the asperity (Fig. 11). This explains why face-controlled fibres can be expected at the rims of fringes where α is low, even on rough core-objects. Asperities with an angle β of 180° are flat surfaces so that fibre boundaries cannot be locked. Very pointed asperities with an angle β approaching 0° will be able to lock fibres irrespective of α.

4. Discussion

Modelling of fibre growth in strain fringes with the program 'Fringe Growth' shows that a strain analysis based on the assumption that the long axis of displacement-controlled fibres is parallel to the extensional ISA (Durney and Ramsay, 1973; Ramsay and Huber, 1983; Ellis, 1986) is only applicable in some very special cases. Our modelling supports the assumption of Urai et al. (1991) and Aerden (1996) that displacement-controlled fibres follow points on the core-object surface. Rotation of core-object and fringe with respect to each other influences fibre patterns (Figs. 1a and 9). This influence must be taken into account before fringes can be used in kinematic analysis. The method of Aerden (1996) to interpret object-centre paths and relative object-fringe rotation for strain fringes is supported by our simulations, even though he interpreted only displacement-controlled fibres. Simulations with the model 'Fringe Growth' can explain the occurrence of both face- and displacement-controlled fibres in one fringe and can reproduce most, if not all, fibre and fringe geometries observed in nature.

Our model confirms the statement of Aerden (1996) that round core-objects do rotate during simple shear deformation with respect to the fringes, since the geometries described in the study presented here correspond to models with a rotating core-object. In nature, it is possible that *both* fringes and the core-object rotate with respect to ISA and to an external reference frame. This can be expected in non-coaxial flow, e.g. simple shear. Fringes will act as rigid objects, and both fringes and core-object will rotate in the shear sense direction, and with respect to each other. This will create fibre geometries similar to those of a rotating core-object with respect to a stationary fringe in the numerical experiments. An extra complication in nature develops because fringes change their shape by growth at the contact with the core-object. Equidimensional fringes will therefore develop towards an elongate shape, and will gradually decrease their rotation rate with respect to ISA; elongate objects rotate more slowly than equidimensional ones if their long axis makes an angle of less than 45° with the flow plane (Ghosh and Ramberg, 1976). The core-object will rotate at constant velocity if equidimensional, or at pulsating rate if elongate. The fibre geometry can store information on such gradients in relative rotation velocity of fringes and core-object (Figs. 1a and 9), and such information may be retrieved from the microstructure.

It is also worth noting that fibre geometries that develop in response to a relative rotation of ISA with respect to the internal reference frame (a line in the rigid fringe or, in our modelling, the computer screen) cannot be easily translated to rotation in an external reference frame. If the internal reference frame (i.e. the fringe) is fixed with respect to the external reference frame (e.g. Earth's surface), the ISA orientation is changing with respect to both reference frames. This could correspond to a change in direction of the stress field. Alternatively the orientation of the fringe is changed with respect to the external reference frame and ISA are fixed in the external reference frame. This could occur by rigid body rotation of the fringes, e.g. in non-coaxial flow. These two cases cannot be easily distinguished by the computer simulations or in nature, since fibre geometries may be identical. However, further modelling may lead to recognition of specific relative rotation histories of ISA and fringe that are typical for one case or the other.

A single fibre may have displacement-controlled and face-controlled oriented segments along its length, which will be difficult to distinguish in natural examples. In fact, the terms 'displacement-controlled' and 'face-controlled' are end-member models, and fibres or sections of fibres can have orientations that fit neither of the two. It is therefore unrealistic to speak of 'face-controlled fringes' or 'displacement-controlled fringes' except in some special situations. In particular core-objects with pronounced corners produce very complex fibre patterns during non-coaxial progressive deformation. In these cases not even the shape of the fringe itself reflects the opening path, but is strongly influenced by the geometry of the core-object (Figs. 1b and 8).

For most natural examples, trial and error simulations can be carried out with 'Fringe Growth' to produce the observed fibre and fringe geometry and to evaluate the object-centre path and relative core-object fringe rotation. Because of the large number of possible geometries, this is a major project that is now in progress. A new program is also being developed to calculate the core-object paths and relative core-object fringe rotation directly from images of natural examples of strain fringes.

5. Limits of the computer program

The 'Fringe Growth' program can model fibre growth in fringes, but obviously not all factors governing fibre growth in nature can be included. The following limitations of the program may be important.

1. The model incorporates the nucleation of new crystals next to the core-object at the rims of the fringe. No nucleation takes place further inside the fringe. A new nucleus is inserted if the growing grain next to the core-object has reached a certain width or if the distance from the fringe to the core-object is larger than half this width. This width can be set by the user and changed during a simulation. In nature the initiation of new nuclei is a function of oversaturation, seeds, opening velocity of the fringe and growth velocity of the crystals. Only the last two parameters are included in 'Fringe Growth' so far.
2. If a core-object has very pronounced corners and is rotating, these corners will tend to move over newly grown grains in the fringe. In nature this will either stop the rotation of the core-object or the fringe, or parts of the fringe will be fractured or dissolved. In the present version of 'Fringe Growth' the rotation of the core-object or the fringes can be stopped if the core-object corners move into the fringe but the grains cannot be dissolved.
3. The present version of 'Fringe Growth' is purely kinematic. It models growth of grains into an open space and is based on the crack–seal process. Growth of fibres in strain fringes might also take place by a growth process accompanying pressure solution. If the fringe is opening more slowly than growth of crystals in the fringe, and if an incremental opening step of the fringe is smaller than the growth step of the slowest growing crystal in the fringe, no 'crack' may develop between the core-object and the fringe (Mügge, 1928). The material for the growth of the fibres will be transported by diffusion along the grain boundaries and will precipitate at the interface of core-object and fringe. This interface can support a differential stress, in contrast to the fluid in an open crack. Fibre geometries probably will not change dramatically by this process, since the present version of 'Fringe Growth' can already produce natural looking fringes. The tracking capability of the fibres might be enhanced however, and this has to be tested with a version of 'Fringe Growth' that includes differential stress effects.
4. The rotation and opening rates are treated as independent. In a real, dynamic system they are probably not independent. A future version may include this dependence and thus reduce the number of possible fringe and fibre geometries.

6. Conclusions

The computer model 'Fringe Growth' can simulate progressive growth of fibrous strain fringes. Core-object morphology, the roughness of its surface and the growth rate of crystals compared to the opening velocity of the fringes control the growth of displacement-controlled, face-controlled or intermediate fibres. Displacement-controlled fibres develop because the fibre boundaries are locked to outward-pointing asperities on the surface of the core-object. This supports the assumption that these fibres follow points on the core-object surface. Fringes with only displacement- and face-controlled fibres are rare end-members: most of the simulated fringes contain both face- and displacement-controlled fibres and intermediate fibres that change from displacement- to face-controlled growth. The long axis of displacement-controlled fibres does not follow the orientation of the extensional ISA in most cases. Displacement-controlled fibres follow asperities on the surface of the core-object and thus record the opening direction as well as rotation of the core-object and the fringes with respect to ISA and with respect to each other.

The computer program 'Fringe Growth' provides a powerful tool for research and teaching to analyse fibre patterns in antitaxial strain fringes. The program is shareware for Macintosh computers and can be downloaded from the http://veo.elsevier.nl/sg/publish/925 together with QuickTime movies showing progressive fibre growth around different core-objects.

Acknowledgements

We thank Paul Williams and Kyuichi Kanagawa for thoughtful reviews that helped to improve this paper. This project was made possible by a visit of DK to the Epsilon Earth Processes Simulation Laboratory, Dept. of Earth Sciences, Monash University, Clayton (Melbourne), Australia. Marlina Elburg is thanked for the hospitality during the visit. The project was funded by DFG Grant Pa 578/3. We thank Mark Jessell, Janos Urai and Domingo Aerden for their comments and suggestions.

References

Aerden, D.G.A.M., 1996. The pyrite-type strain fringes from Lourdes (France): indicators of Alpine thrust kinematics in the Pyrenees. Journal of Structural Geology 18, 75–91.

Beutner, E.C., Diegel, F.A., 1985. Determination of fold kinematics from syntectonic fibers in pressure shadows, Martinsburg Slate, New Jersey. American Journal of Science 285, 16–50.

Bons, P.D., Jessell, M.W., 1997. Experimental simulation of the formation of fibrous veins by localised dissolution-precipitation creep. Mineralogical Magazine 61, 53–63.

Cox, S.F., Etheridge, M.A., 1983. Crack–seal fibre growth mechanisms and their significance in the development of oriented layer silicate microstructures. Tectonophysics 92, 147–170.

Durney, D.W., Ramsay, J.G., 1973. Incremental strains measured by syntectonic crystal growths. In: DeJong, K.A., Scholten, R. (Eds.), Gravity and Tectonics. Wiley, New York, pp. 67–95.

Ellis, M.A., 1986. The determination of progressive deformation histories from antitaxial syntectonic crystal fibres. Journal of Structural Geology 8, 701–709.

Etchecopar, A., Malavielle, J., 1987. Computer models of pressure shadows: a method for strain measurement and shear sense determination. Journal of Structural Geology 9, 667–677.

Fisher, D.M., Brantley, S.L., 1992. Models of quartz overgrowth and vein formation: deformation and episodic fluid flow in an ancient subduction zone. Journal of Geophysical Research 97, 20,043–20,061.

Ghosh, S.K., Ramberg, H., 1976. Reorientation of inclusions by combination of pure shear and simple shear. Tectonophysics 34, 1–70.

Kanagawa, K., 1996. Simulated Pressure Fringes, Vorticity, and Progressive Deformation. In: De Paor, D.G. (Ed.), Structural Geology and Personal Computers, Computer Methods in the Geosciences, 15, pp. 259–283.

Mügge, O., 1928. Ueber die Entstehung faseriger Minerale und ihrer Aggregationsformen. In: Neues Jahrbuch für Mineralogie, Geologie und Paläontologie, 58A, pp. 303–438.

Pabst, A., 1931. Pressure shadows and the measurement of the orientation in rocks. Journal of the Mineralogical Society of America 16, 55–70.

Passchier, C.W., Trouw, R.A.J., 1996. Microtectonics. Springer, Heidelberg, p. 289.

Ramsay, J., 1980. The crack–seal mechanism of rock deformation. Nature 284, 135–139.

Ramsay, J.G., Huber, M.I., 1983. The Techniques of Modern Structural Geology, 1: Strain analysis. Academic Press, London.

Urai, J.L., Williams, P.F., Van Roermund, H.L.M., 1991. Kinematics of crystal growth in syntectonic fibrous veins. Journal of Structural Geology 13, 823–836.